Biomedicine & Pharmacotherapy 174 (2024) 116508

Contents lists available at ScienceDirect

Biomedicine & Pharmacotherapy

journal homepage: www.elsevier.com/locate/biopha

RNA expression changes driven by altered epigenetics status related to NASH etiology

Daniel Castellano-Castillo [a], Bruno Ramos-Molina [b,*], María Dolores Frutos [c], Isabel Arranz-Salas [d,e,f], Armando Reyes-Engel [g], María Isabel Queipo-Ortuño [a,g,**], Fernando Cardona [g]

[a] Unidad de Gestión Clínica Intercentros de Oncología Médica, Hospitales Universitarios Regional y Virgen de la Victoria, Instituto de Investigación Biomédica de Málaga (IBIMA)-CIMES-UMA, Málaga 29010, Spain
[b] Obesity, Diabetes and Metabolism Laboratory, Biomedical Research Institute of Murcia (IMIB), Murcia 30120, Spain
[c] General and Digestive System Surgery Department, Virgen de la Arrixaca University Hospital, Murcia 31020, Spain
[d] Instituto de Investigación Biomédica de Málaga-Plataforma BIONAND (IBIMA), Virgen de la Victoria University Hospital, Malaga University, 2ª Planta, Campus Teatinos S/N, Málaga 29010, Spain
[e] Department of Human Physiology, Human Histology, Anatomical Pathology and Physical Education, Malaga University, Málaga 29010, Spain
[f] 11 Department of Anatomical Pathology, Virgen de la Victoria Hospital, Málaga, Spain
[g] Departamento de especialidades Quirúrgicas, Bioquímica e Inmunología, Facultad de Medicina, Universidad de Málaga, 29010, Spain

ARTICLE INFO

Keywords:
Epigenetics
NASH
obesity
ATACseq
chromatin openness
liver

ABSTRACT

Non-alcoholic fatty liver disease (NAFLD) is a growing health problem due to the increased obesity rates, among other factors. In its more severe stage (NASH), inflammation, hepatocellular ballooning and fibrosis are present in the liver, which can further evolve to total liver dysfunction or even hepatocarcinoma. As a metabolic disease, is associated to environmental factors such as diet and lifestyle conditions, which in turn can influence the epigenetic landscape of the cells, affecting to the gene expression profile and chromatin organization. In this study we performed ATAC-sequencing and RNA-sequencing to interrogate the chromatin status of liver biopsies in subjects with and without NASH and its effects on RNA transcription and NASH etiology. NASH subjects showed transcriptional downregulation for lipid and glucose metabolic pathways (e.g., ABC transporters, AMPK, FoxO or insulin pathways). A total of 229 genes were differentially enriched (ATAC and mRNA) in NASH, which were mainly related to lipid transport activity, nuclear receptor-binding, dicarboxylic acid transporter, and PPARA lipid regulation. Interpolation of ATAC data with known liver enhancer regions showed differential openness at 8 enhancers, some linked to genes involved in lipid metabolism, (i.e., FASN) and glucose homeostasis (i.e., GCGR). In conclusion, the chromatin landscape is altered in NASH patients compared to patients without this liver condition. This alteration might cause mRNA changes explaining, at least partially, the etiology and pathophysiology of the disease.

1. Introduction

Non-alcoholic fatty liver disease (NAFLD) is a chronic liver disease whose rate and incidence is increasing worldwide, as it is frequently associated with obesity [1,2]. This metabolic disease ranges from simple steatosis (excessive lipid accumulation in the liver) to non-alcoholic steatohepatitis (NASH), when inflammation and hepatocellular ballooning, and sometimes liver fibrosis, is present [3]. Additionally, NASH is associated to an increased risk of developing advanced chronic liver disease (cirrhosis) or even hepatocarcinoma [1,3]. Despite the relative high prevalence of NASH in the overall population, this liver condition remains understudied at the molecular level. Consequently, deep research is necessary to fully understand the etiology of the disease, for a better and less invasive prognosis and for an effective treatment.

Abbreviations: NAFLD, Non-alcoholic fatty liver disease; NASH, Non-alcoholic steatohepatitis; ATAC-seq, Assay for Transposase-Accessible Chromatin; SREBP, Sterol Regulatory Element-Binding Protein; PPARA, Peroxisome Proliferator-Activated Receptor Alpha.

* Corresponding author.
** Corresponding author at: Departamento de especialidades Quirúrgicas, Bioquímica e Inmunología, Facultad de Medicina, Universidad de Málaga, 29010, Spain.
E-mail addresses: bruno.ramos@imib.es (B. Ramos-Molina), iqueipo@uma.es (M.I. Queipo-Ortuño).

https://doi.org/10.1016/j.biopha.2024.116508
Received 11 January 2024; Received in revised form 22 March 2024; Accepted 27 March 2024
Available online 4 April 2024

Due to its metabolic basis, lifestyle habits such as diet, sedentarism, obesity and other metabolic diseases can influence this liver condition [1,2]. As such, the epigenetic mechanisms emerge as an interesting landscape to unravel the molecular mechanisms involved on NAFLD physiopathology. Indeed, epigenetic mechanisms such as DNA methylation (present in cytosines residues of CG dinucleotides) or histone modifications can be modulated by lifestyle and environmental factors including metabolic status, diet and gut microbiota [4,5]. These epigenetic mechanisms rely on substrate availability coming from central metabolic pathways such as acetyl-CoA [4]. Besides, these metabolic intermediaries can regulate the enzymatic activity of some epigenetic modifiers and therefore modulate the epigenome (e.g., alpha-ketoglutarate, fumarate, succinate) [6,7]. Other metabolic intermediaries (either endogenous or derived from gut microbiota) have recently been shown to modify histone residues and are capable of modulating the epigenome (e.g., lactate, propionate, butyrate or iso-butyrate) [8]. Therefore, the epigenetic landscape emerges as a complex fine-tune mechanism, which in turn controls chromatin and can eventually modulate gene expression.

Due to sample limitation and the big complexity of the epigenetic landscape (multiple modifications can be present on a single histone), assay for Transposase-Accessible Chromatin sequencing (ATAC-seq) has emerged as a surrogate to assess chromatin status [9]. This assay relies on the capacity of a transposase (TN5) pre-loaded with sequencing primers to cut and add those primers in open regions of the genome [9]. Therefore, by using this technology we can determine genome-wide open and close regions of the genome.

In this work, we interrogate chromatin status of NASH livers in comparison to those without NASH by ATAC-seq. Moreover, we performed whole transcriptome sequencing to relate possible changes in chromatin structure in NASH with transcriptional changes in such condition.

2. Material and methods

2.1. Study participants and sample collection

In this study we included 13 patients with obesity that underwent bariatric surgery at the Virgen de la Arrixaca University Hospital (Murcia, Spain) between 2020 and 2021. Inclusion criteria comprised signed informed consent, age between 18 and 65 years, a body mass index (BMI) of $\geq$35 kg/m2 with significant obesity-related comorbidities, and a minimum obesity duration of $\geq$5 years. Exclusion criteria were evidence of liver disease other than NAFLD (including viral hepatitis, medication-related disorders, autoimmune disease, hepatocellular carcinoma, hemochromatosis, Wilson's disease, familial/genetic causes), a previous history of excessive alcohol use (>30 g daily for men and >20 g daily for women), treatment with any drugs potentially causing steatosis, such as tamoxifen, amiodarone, and valproic acid, or subjects who declined to participate. Study groups were defined based on the histological evaluation of liver biopsies according to the SAF (Steatosis, Activity, Fibrosis) [10] classification system as: 1) non-NASH (liver without any histological alteration or with simple steatosis); and 2) NASH with or without fibrosis. Table S1 describes liver scoring used for the diagnosis of the study population. Fig S1 shows the representative liver section for control patients and those with NASH.

The study was performed in agreement with the Declaration of Helsinki according to local and national laws and was approved by the Ethics and Clinical Research Committees of the Virgen de la Arrixaca University Hospital (ref. number 2020–2-4-HCUVA).

2.2. Biochemical evaluation

Blood samples were collected from study patients after an overnight fast of at least 12 h and serum was separated by centrifugation. The determination of glucose, total cholesterol, high-density lipoprotein cholesterol (HDLc), low-density lipoprotein cholesterol (LDLc), triglycerides and alanine aminotransferase (ALT) was carried out using the Cobas Analyzer c702 (Roche). Insulin levels were measured using the Cobas Analyzer e801 (Roche). Insulin resistance was determined by the Homeostasis Model Assessment of Insulin Resistance (HOMA-IR) index, and was calculated as insulin (μU/ml) x glucose (mmol/L)/22.5.

2.3. Liver biopsies collection and sample processing

Intraoperative wedge liver biopsies from patients that underwent bariatric surgery patients of at least 1 cm in depth were obtained. One section of the liver biopsy was snap-frozen and stored at −80°C and the other was formalin-fixed and paraffin-embedded for histological assessment. Paraffin-embedded 5 μm sections of human liver biopsies were stained for hematoxylin and eosin (H&E), Masson trichrome, Periodic acid–Schiff (PAS), Perls and reticulin staining. All biopsies were reviewed and scored by trained liver pathologists from the Virgen de la Arrixaca University Hospital and the Pathology Platform of the Biomedical Research Institute of Murcia (IMIB) to determine liver status.

2.4. ATAC sequencing and analysis

For ATAC sequencing, snap-frozen liver biopsies were minced and processed with pre-cold lysis buffer (10 mM TrisCl pH7.4, 10 mM NaCl, 3 mM MgCl2, Igepal CA-630 0.1%, Tween 20 0.1%) and Dounce (15 strokes with loose pestle and 15 strokes with tight pestle) on ice after that they were incubated on ice for 5 minutes. To stop lysis, pre-cold PBS+1% BSA was added and the samples were transferred to a 15 ml falcon tube and centrifuged at 500xg for 5 minutes using a swinging bucket centrifuge. After carefully removing the supernatant, nuclei were resuspended in pre-cold PBS+1% BSA and counted using a hemocytometer. 10,000 nuclei were then passed to a 96-well plate format and centrifuged as described before to remove the supernatant. The nuclei were then resuspended in 20 μl tagmentation buffer (4 μl 5xTAPS-DMF buffer (50 mM TAPS-NaOH, 25 mM $MgCl_2$, 50% DMF (v/v) pH 8.5), 3 μl TN5, 0.1 μl of 2% digitonin stock, 12.9 μl of nuclease-free H_20) and tagmentation was performed in a thermocycler at 37ºC for 30 minutes. After the incubation, the tagmentation was stopped by adding DNA binding buffer (Zymo DNA clean and concentrator kit, EGD4014200). DNA fragments were then purified in columns following the manufacture's instruction (Zymo DNA clean and concentrator kit) and eluted in 20 μl of H_20. ATAC libraries were then finished by amplifying the tagmented DNA fragments and indexed (Nextera compatible indexing) by adding PCR mixture (2.5 μl of 25 μM stock primer P5 and P7, 10 μl Kapa HF buffer, 1.5 μl Kapa dNTPs mix, 1 μl Kapa HiFi Hot Start DNA polymerase and 12.5 μl H_20) in a thermocycler. ATAC libraries were then purified using AMPure beads, checked for fragment size distribution, and sequenced in a NovaSeq 6000 instrument (PE 75 bp) (Illumina).

After sequencing raw, data was trimmed using the *cutadapt* function in *TrimGalore* software. Cleaned fragments were then aligned against the Hg38 reference genome with the help of the bioinformatic package *Subread* (*Subread-align* function). Peak calling was performed using *Seacr* aligner package for broad peaks. Peak annotation and visualization were performed using the R packages *ChIPseeker* and *EnrichedHeatmap*, respectively. Differential enrichment analysis was performed for peaks spanning promoter regions and gene bodies using the R package DESeq2. Afterwards, differentially enriched peaks (pval<0.05) were analyzed and visualized for Pathway enrichment using *clusterProfiler* in R studio.

For the differentially enriched enhancer analysis, raw counts of intersected pre-defined human hepatocyte enhancer regions (http://www.enhanceratlas.org/database) were obtained, and differential enrichment analysis was performed as described before.

Motif enrichment analysis of the gene intersection between differentially enriched peaks in the ATAC-seq and differentially expressed genes in the RNA-seq was conducted using the *findMotifsGenome.pl*

function in the software *HOMER*.

2.5. RNA sequencing and analysis

Snap-frozen liver biopsies were used for RNA extraction. cDNA libraries (provided by Novogene sequencing service) were sequenced using a NovaSeq 6000 instrument (PE150 bp) (Illumina). After sequencing, alignment was performed using the human genome hg38 as reference and the *Subread* software (*Subread align* function). Gene counts were obtained using the *featureCounts* function in the *Subread* software. For differential gene expression analysis, DESeq2 was used (pval<0.05). Pathway enrichment analysis and visualization of differentially expressed genes were performed using the *clusterProfiler* R package. Integration and final analysis of the RNA-seq and ATAC-seq datasets were conducted in R Studio.

2.6. Statistical analyses

Comparisons of clinical and anthropometric variables between groups were calculated using the Mann-Whitney U-test test for non-normal distribution variables. Values were statistically significant when p< 0.05. The analyses were performed with SPSS (Version 15.0 for Windows; SPSS).

3. Results

3.1. Genome-wide chromatin accessibility profile

Anthropometric and biochemical variables are depicted in Table 1. Genome-wide chromatin accessibility profile was carried out by peak calling in DNA samples isolated from liver biopsies of both controls (non-NASH) and NASH patients (Fig. 1A). We observed that genomic features marked with a peak display similarly for all the liver tissue samples analyzed, (Fig. 1B, Fig S2), as well as the plot average profile (Fig S3). Additionally, we observed that chromatin accessibility was predominant at promoter regions and gene body as expected [11], being all the genomic distribution similar among the samples (Fig. 1C). This overall chromatin accessibility similarity observed between samples, also confirmed by PCA analysis (Fig S4), is an indication of technical soundness and quality data robustness, which is expected since all the samples correspond to the same type of biological sample.

Table 1
Anthropometric and biochemic variables of the study population.

	Control (n=7)	NASH (n=6)	Pval
Age (years)	39.5±7.2	45.6±6.9	0.138
Gender (M/F)	4/3	3/3	1.000
BMI (Kg/m^2)	46.8±9.2	45.2±6.7	0.945
Waist (cm)	129.8±13.5	134.0±10.6	0.445
Glucose (mg/dL)	94.1±6.2	101.5±21.5	0.534
Insulin (UI/ml)	14.8±9.8	22.4±6.5	0.051
HbA1c (%)	5.2±0.3	5.5±0.3	0.181
HOMA-IR	3.3±2.0	5.8±3.1	0.051
TG (mg/dL)	125.7±83.9	126.6±71.0	0.836
Chol (mg/dL)	161.1±16.5	182.6±75.9	0.295
HDL-C (mg/dL)	45.4±15.6	45.8±12.9	0.836
LDL-C (mg/dL)	96.0±13.7	111.5±58.4	0.295
ALT (units/L)	25.2±6.9	31.1±11.7	0.628
GGT (units/L)	37.8±38.9	34.3±15.2	0.836

Abbreviations. Male (M); female (F); body mass index (BMI); glycated hemoglobin A1c (HbA1c); Homeostatic model assessment of Insulin Resistance (HOMA-IR); triglycerides (TG); total cholesterol (Chol); high-density lipoprotein cholesterol (HDL-C); low-density lipoprotein cholesterol (LDL-C); alanine transaminase (ALT); gamma glutamyl transferase (GGT). Pvalue for non-parametric Mann-Whitney's U test, and Chi-square test for gender distribution analysis between groups.

3.2. Top chromatin accessibility genome sites in NASH are located on lipid-related genes

After passing through the quality check, we conduct a comprehensive bioinformatic analysis of the chromatin accessibility data, with a particular emphasis on genes that are predominantly accessible in the liver. It is known that chromatin accessibility is positively correlated to gene expression, and that ATAC peaks can predict gene expression profile. Differential enrichment (DE) analysis using tools such as DESeq2 or edgR are used to search for differentially open regions in ATAC-sequencing, though these tools where originally designed for transcriptional analysis. However, the use of this software for peak differential analysis requires the creation of a consensus open region frame between samples, which can impact DE results [12]. To overcome this limitation and in addition to the DE analysis performed, in this work we analyzed the top 3000 ranked peaks for each condition (controls and NASH) with the aim of assessing if top chromatin accessibility (most active chromatin sites) is present in a different set of genes. After ranking these 3000 top genes we performed pathway enrichment analysis, finding that the most prevalent (ranked by p adjusted value) pathways for top open genes in the control group mostly classified for pathways related to main cell processes, such as serine/threonine kinase activity, mRNA metabolism, protein metabolism in endoplasmic reticulum or regulation of transferase activity (Fig. 1D). Contrary to the control group, the top 3000 genes in NASH subjects are part of pathways related to lipid metabolism as cholesterol metabolic process, glycerolipid metabolic process, regulation of lipid metabolic process or phospholipid metabolic process, among some pathways related to topologically incorrect protein response or response to unfolded protein processes (Fig. 1D). This is also observed when we enriched for KEGG and Reactome terms. For instance, we found that in NASH subjects the most prevalent pathways, compared to control subjects, were involved in pathways such as AMPK signaling, lysosome, apoptosis, GLUT4 translocation to plasma membrane, regulation of cholesterol biosynthesis and gene expression activation by SREBP and PPARA activate expression, among others (Table S2). Overall, we observed that chromatin accessibility in liver tissue differs between controls and NASH subjects when the top 3000 ranked open peaks in genes are considered.

3.3. Liver transcriptional profile in NASH

After chromatin accessibility analysis we performed transcriptional analysis of liver biopsies. Before differential enrichment analysis between groups, we quantified and plotted using PCA analysis the whole population, in which we confirmed all datasets were within expected variance and all the samples were considered to pass quality check (Fig S5). We found that over 1000 genes were transcriptionally deregulated (pval<0.05) in the NASH versus the control group (Fig. 2A and Table S4). After conducting a differential expression analysis, we subjected the deregulated genes to pathway enrichment analysis. We observed that the deregulated pathways could potentially contribute to the observed etiology of NASH, as they are involved in lipid and glucose metabolism or cell fibrosis (Table S4 and Fig S6). Additionally, we performed Generally Applicable Gene-set Enrichment (GAGE) analysis, which takes into account total pathway perturbations with the aim to increase sensitivity and robustness of possible deregulated pathways over conventional DE-based pathways enrichment analysis. Notably, we found that 7 pathways (KEGG ontology) were transcriptionally upregulated in NASH (pval<0.05), being related to immune system processes, cell adhesion and actin cytoskeleton (Table S5). GAGE analysis also showed that 26 pathways were transcriptionally down represented in NASH, which were mainly related to lipid metabolism and transport, TCA cycle, cytochrome P450 processes, steroid hormone and bile acid metabolism, PPAR signaling, amino acid metabolism, starch and sucrose metabolism or peroxisome, among others (Table S5). Therefore, these de-regulated pathways might partially explain the etiology in NASH (e.

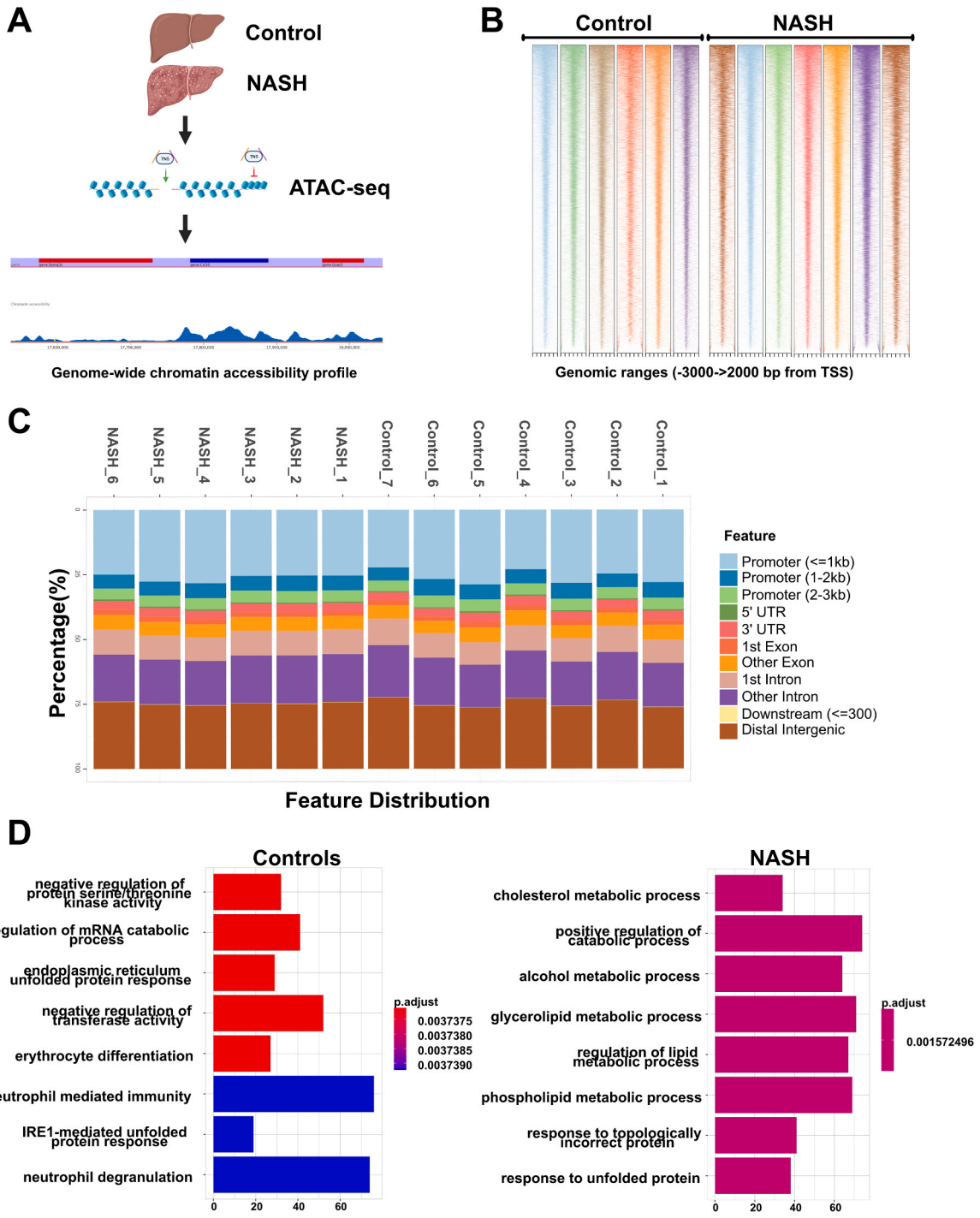

Fig. 1. Liver chromatin profile in NASH. (A) ATAC-sequencing workflow carried out to profile chromatin accessibility in human liver tissue of patients with or without NASH; (B) ATAC-seq reads around transcription start site (TSS) for all annotated genes in the whole population of study shows similar TSS reads distribution along patients; (C) Genomic distribution for called ATAC-peaks demonstrates most of the peaks (open regions) are located in promoters and gene body; (D) Pathway enrichment analysis of the top 3000-ranked ATAC-peaks (open regions) shows differential enrichment in control and NASH liver biopsies, being highly enriched in GO terms for lipid-related pathways in NASH compared to control subjects.

g., lipid accumulation, inflammation, fibrosis, or liver insulin resistance).

3.4. Chromatin accessibility deregulation in NASH

For a robust analysis of chromatin accessibility in NASH compared to the control group we performed differential analysis of ATAC-seq peaks between both groups. We found 4979 differentially accessible regions in liver tissue of NASH patients compared to the controls (Fig. 2B). To assess if these deregulated chromatin regions could in part explain the differential transcription profile observed between groups, we looked for genes deregulated at both chromatin and transcriptional levels. We found 229 genes that were deregulated for chromatin accessibility and transcription, which represents more than 21% of DE transcripts (Fig. 2C and Table S6). To understand the potential role of such deregulated genes in NASH, we performed Motif Enrichment Analysis (MEA) and

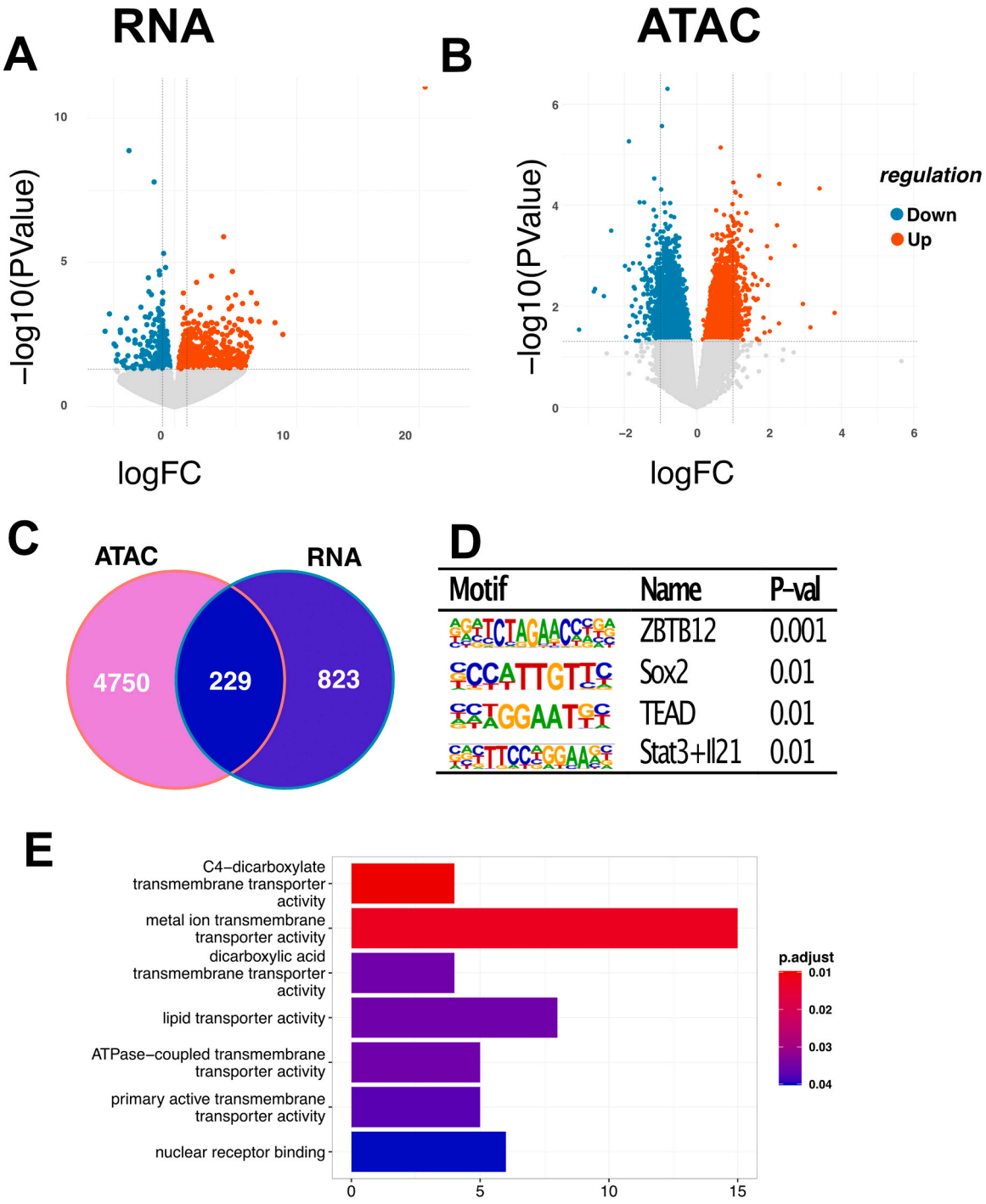

Fig. 2. RNA and ATAC sequencing integration of differentially expressed/enriched (DE) transcripts and peaks. (A) Volcano plot of DE peaks between NASH and control subjects in liver; (B) Volcano plot of liver DE transcripts between NASH and control subjects. (C) Venn plot of the intersection between DE transcripts and peaks shows 229 genes both de-regulated at chromatin and mRNA levels; (D) Motif Enrichment Analysis (MEA) for the DE ATAC peaks in genes de-regulated both, transcriptionally and at the chromatin level; (E) Pathways enrichment analysis (GO terms) of the 229 genes de-regulated at the chromatin and transcript levels.

pathway enrichment analysis of those genes. As shown in Fig. 2D, ATAC peak sequences for those 229 genes showed Motif enrichment for factors such as ZBTB12, Sox2, TEAD, STAT3+Il21. Pathway enrichment analysis of the same set of genes showed that they were part of pathways involved in lipid accumulation in NASH such as lipid metabolism and transport, regulation of expression and lipid metabolism by PPARA or dicarboxylic acid transporter (Fig. 2E and Table S7).

3.5. Chromatin de-regulation in enhancer positions

Near 35% of differentially open peaks were annotated to non-promoter and gene body regions (Fig. 3A). Therefore, we used liver-specific enhancer positions using as reference the liver enhancer annotation found in enhancer atlas database [13]. To do so, we intersected the reference liver enhancer bed file with our reads and search for differentially open enhancers using DESeq (Fig. 3B). We found 8 differentially open peaks between the control and the NASH group which were linked for the genes (experimentally curated) depicted in

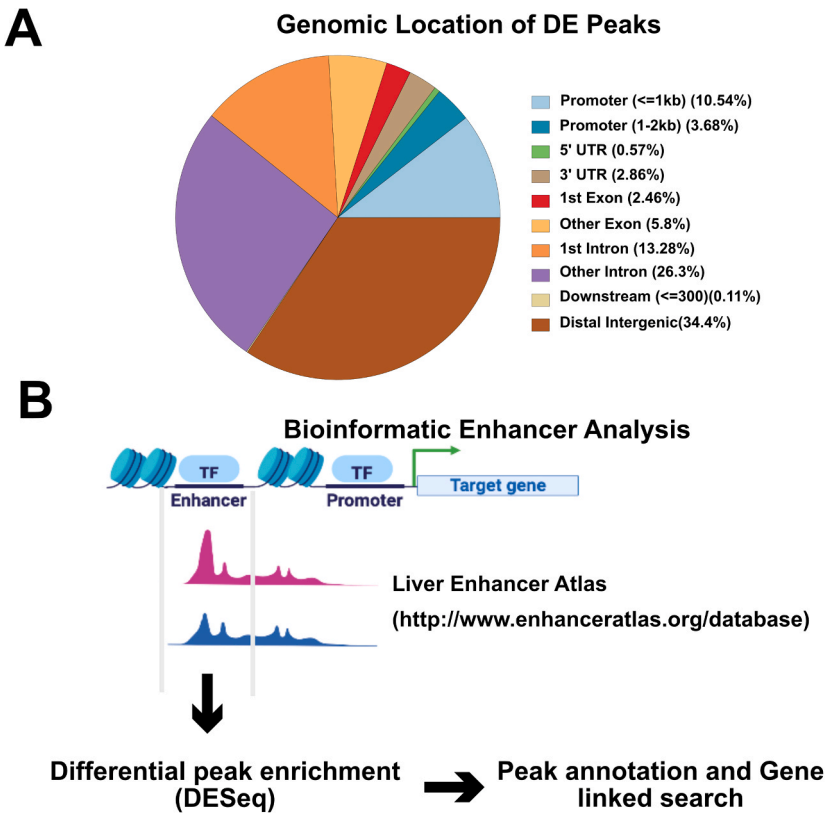

C

Chr	dbSUPER_ID	Gene linked (dbSUPER)	GeneCards_ID	Gene Linked (GeneCards)	FC
chr16: 1392820-1392910	SE_65650	UBE2I			1.76
chr15: 77916420-77924650	SE_05045 SE_07079	HMG20A LINGO1			0.31
chr17: 80052630-80053190	SE_25146	FASN	GH17I082094	FASN, DUS1L, SLC25A10, ASPSCR1, PCYT2, DCXR, LRRC45, FOXK2, GCGR, MRPL12, HEXD, piR-58439	-0.85
chr1: 1675590-1675680	SE_11679	SLC35E2			2.65
chr12: 6941080-6941220					1.11
chr16: 1392280-1392520	SE_65650	UBE2I			0.85
chr11: 65386720-65386960					0.53
chr12:38536310-38537070			GH12I038142	LOC107984469, ENSG00000287442, HSALNG0090407, ALG10B	-0.81

Fig. 3. Chromatin analysis of liver enhancer consensus between NASH and control subjects. (A) Pie chart showing the genomic distribution of DE ATAC peaks; (B) Bioinformatic workflow for the differential enhancer enrichment performed between groups; (C) Annotation for differentially enriched enhancers between NASH and control patients.

Fig. 3C. Thus, according to dbSUPER enhancer database [14] enhancer SE_656550 is linked to UBE21; SE_05045 to HMG20A; SE_07079 to LINGO1; SE_25146 to FASN; and SE_11679 to SLC35E2. Additionally, GeneCards database provides further information, for instance enhancer SE_25146 is also related to genes involved in lipid and /or glucose metabolism such as DUS1L, SLC25A10, ASPSCR1, PCYT2, DCXR, LRRC45, FOXK2, GCGR, MRPL12, HEXD, piR-58439 in addition to FASN.

4. Discussion

In this manuscript we interrogate chromatin and transcriptional profiles in liver tissue samples of patients with obesity, comparing those with NASH and those without NASH (defined as controls) in order to gain knowledge about the etiology of this prevalent chronic liver disease. Overall, we found clinically relevant information pointing out that chromatin configuration could contribute to NASH disease, and therefore epigenetic-based pharmacological approaches in which chromatin configuration can be modulated are potential strategies to be regarded [15]. Drugs modulating key epigenetic enzymes have been used for the treatment of some diseases such as cancer. For instance, azacytidine, a DNA methyltransferase inhibitor, has been successfully used for the treatment of acute myeloid leukemia or myelodysplastic syndrome [16,17]. Another example are the histone deacetylase inhibitors romidepsin and belinostat, which have been approved for the treatment of cutaneous T-cell lymphoma and acute myeloid leukemia [18,19].

Chromatin openness is currently assessed using ATAC-seq analysis [9]. In this work, we have performed for the first time an ATAC-seq together with a RNAseq analysis in human liver tissue samples from

patients with obesity and different liver status, directly comparing liver tissue from NASH subjects and those without NASH. We found that the most open regions in promoters in NASH are found in genes that are part of important pathways for NASH etiology, compared to the control group in which top open regions are found in promoters of genes related to constitutive cell processes. As known, NASH is characterized by lipid accumulation, inflammation and, in the advance stages of the disease, liver fibrosis [3]. In accordance, we found that the most significant pathways found in NASH livers were characterized by open regions for genes involved in pathways such as "cholesterol metabolic process", "glycerolipid metabolic process" or "phospholipid metabolic process". We also found pathways such as "AMPK signaling", "GLUT4 translocation to plasma membrane" or "RHO signaling", which are related to insulin action, and that could indicate the presence of hepatic insulin resistance in NASH as previously described [20–23]. We also revealed enrichment in "lysosome" pathway, lysosomal dysfunction can contribute to NASH etiology [24], or "FOXO signaling" that is known to coordinates glucose and lipid metabolism and its function seems to participate in liver disease in mice [25,26]. Interestingly, we found that the top open regions in NASH were also present in two main pathways for lipid regulation: SREBP and PPARA, which are key transcription factors that regulates cholesterol and lipid metabolism and that contributes to the etiology of liver disease [27–29]. For instance, it has been shown that activation of PPARA in diet-induced obese mice can reverse inflammation and fibrosis in liver, while deletion of SREBP1c in mice aggravates liver steatosis by activating lipogenesis and inhibiting lipolysis [29,30]. Therefore, since chromatin configuration can regulate gene transcription [31], this suggest that deregulation of chromatin in NASH could be contributing to the disease.

Furthermore, we characterized the transcriptional profile of liver tissue samples to establish the potential role of chromatin configuration in the transcriptional profile in NASH conditions. We found over 1000 transcripts differentially abundant in NASH compared to the control group, which might be partially driven by changes in cell composition in liver during NASH [32,33]. Thus, among the up-regulated genes, we found several ones that were part of pathways that are related to immune system processes and cell fibrosis, such as actin metabolic processes and heart related terms, which could be related with stellate cell activation towards myofibroblast-like cells that, a well known driver of liver extracellular matrix accumulation during NASH. This is in line with the etiology of NASH, which is characterized by increased inflammation and fibrosis [34]. A transcriptomic analysis between different NAFLD degree was performed previously [35]. They found milder transcriptomic differences between liver biopsies with steatosis and NASH (all the biopsies with fibrosis) in comparison with healthy liver biopsies. We found overlap of 30 genes, as for example GPNMB, AKR1B10, DES, APOD or RORC. In our comparison, we are analysing subjects with NASH (fibrosis present in 3/6 subjects) and a control group without NASH but some degree of steatosis. Additionally, while they studied subjects with obesity (BMI near 30) we had patients with severe morbid obesity for both study groups. These differences might explain the differences seen in our transcriptional profile for both groups, since we also observed alterations in pathways related to lipid metabolism, immune cells, and inflammation. By contrast, we observed alteration in pathways related to glucose homeostasis, insulin resistance or actin pathways.

Next, we aimed to interrogate whether those transcriptional changes could be induced by epigenetic changes, especially those related to chromatin conformation. In order to do so, we integrated both datasets, finding that more than 20% of transcriptionally deregulated genes (229) had chromatin openness differences in the promoter of NASH livers compared to those used as controls. When we underwent these 229 genes to pathway enrichment analysis we observed that they are part of important pathways to explain the etiology of NASH including lipid transport and metabolism or nuclear receptor activity (related to PPAR signaling), which is known to regulate lipid metabolism [36]. As examples of genes de-regulated at the chromatin and transcript level we found PPARGC1A, ABCA1, FOXO1, SLC13A3, ABCB11 and ARNTL, among many others. PPARGC1A, a co-regulator of PPARA, and that is known to control fatty acid oxidation and glucose metabolism (gluconeogenesis) in liver [37]. In human cohorts, PPARGC1A rs8192678 polymorphism has been related to steatosis and steatohepatitis degree, while in mice models of NAFLD PPARGC1A is decreased and the pathway SIRT1/PPARGC1A has been proposed as a possible target to treat the disease [38,39]. Another interesting gene deregulated at both chromatin and transcriptional levels is FOXO1, which as described before is known to regulate glucose and lipid metabolism and that has been described to be involved in liver disease in mice [25,26]. Moreover, ABCA1 knockout in mice, which is a cholesterol efflux transporter and is key for the formation of HDL particles, is known to produce lipid storage in several tissues specially in those with high lipid turnover like liver [40]. By contrast, recent liver-specific knockout of ABCA1 showed impaired *de novo* lipid synthesis in liver, protecting against lipid accumulation in the liver by mean of a insulin resistance process independent of glucose deregulation [41]. SLC13A3 is a di/tricarboxylic acid transported for succinate, alpha-ketoglutarate and citrate and therefore can be key for lipid synthesis. Though is not known its role in NASH, the paralog SLC13A5 has been related to liver steatosis and citrate accumulation promotes steatosis and steatohepatitis by fueling *de novo* lipogenesis [42]. In a study carried out in mice, the authors demonstrated that bile acid export ablation mediated by Bsep or ABCB11 (Mdr2) promotes liver damage and inflammation impairment in lipopolysaccharide (LPS) elimination trough bile acid secretion [43]. A PPARA signaling factor, ARNTL (which integrates metabolism and circadian clock) has been related to liver disease. Thus, knock-out of ARNTL causes early obesity in mice fed at high fat diet but prevents from liver steatosis [44]. Another study, showed that overexpression of ARNTL protects liver from fibrosis by inhibiting the pro-fibrogenic phenotype of stellate cells in an IDH1/α-KG dependent mechanism [45]. Therefore, we observed that transcriptional changes that might be driven by epigenetic changes are related to lipid metabolism in liver biopsies of NASH patients, which could be contributing to the disease.

Since we focused on ATAC-peak changes located at gene promoters and gene body, we further investigate the possible chromatin changes located in other genomic regions. To perform that, we intersected ATAC-seq data with known liver enhancer atlas [13]. We found 8 peaks inside enhancers differentially open at the chromatin level, located at Chr16 (2), Chr15, Chr17, Chr1(2), Chr12 (2). For instance, enhance position ID SE_05045 is linked to the chromatin remodeler HMG20A, and has been involved in glucose metabolism through is action over LSD1 [46]. Another differentially regulated enhancer was SE_65650, which is linked to UBE2I, a protein highly expressed in hepatocellular carcinoma (HCC). Inhibition of UBE2I appears to be associated with the regulation of liver lipid storage and liver disease [47]. Specially interesting is the deregulation of enhancer SE_25146 that is linked to fatty acid synthase (FASN), key enzyme in the de-novo biosynthesis of lipids. This enzyme is a possible pharmaceutical target to treat NASH and its inhibition has been shown to reduce lipid storage, fibrosis and inflammation in experimental NASH models and in NASH patients [48,49]. Other genes linked to this enhancer are: the mitochondrial transporter SLC25A10 which has also been related to NASH [50,51]; ASPSCR1 an UBX containing domain factor that is known to regulate glucose homeostasis by regulating the subcellular location of GLUT4 [52,53]; the phosphoethanolamine synthesizer PCYT2 which inhibition has been shown to produce liver steatosis and insulin resistance in mice [54,55]; DCXR for what a low expression has been shown to be related to bad prognosis in HCC [56]; FOXK2, an insulin-responsive transcription factor that regulates metabolism following insulin signaling [57]; or the glucagon receptor GCGR which activation can ameliorate liver steatosis and NASH [58].

Therefore, one epigenetic change in one enhancer position could have a great impact on cell function, pointing out the importance that these mechanisms can have on the incidence, development and

therapeutics of NASH. On the other hand, the fact that the epigenetic regulation can coordinate the transcription of a wide frame of transcripts makes interesting the possible development and application of epigenetic-based therapies in which deleterious reversion could have a deeper efficiency. New studies either based on pharmacological modulation (epigenetic-based drugs) [15], nutritional or microbiome modulation (due to the big impact the nutrition or bioactive compounds have over the epigenetic landscape) [5,8,31,59] or by mean of molecular manipulation (using dCAS9 fused to chromatin modifiers) [60–62] are necessary to fully disentangle the role that the epigenetic mechanisms have in this disease and to develop new therapeutical approaches.

5. Conclusions

In conclusion, in this study we demonstrate that NASH is characterized by altered epigenetic regulation, more specifically chromatin openness, which could partially explain alterations in the transcriptional profile of these patients. These alterations are in genes (both promoter and gene body) and enhancers that can in part explain the etiology of the disease (e.g., pathways related to lipid metabolism, lipid transport or PPARA signaling, among others). Moreover, this work points out the potential role that the epigenetic mechanisms may play in the etiology of NASH, though emphasizing the need of further studies to understand such epigenetic mechanisms and to be able to regulate those by means of functional diets, intake of bioactive compounds, gut microbiome-based therapies, or new pharmacological approaches.

Ethics approval and consent to participate

The study was approved by the Ethics and Clinical Research Committees of the Virgen de la Arrixaca University Hospital, ref. number 2020–2–4-HCUVA). Written informed consent was obtained from all the study participants.

Author contribution

F.C., M.I.Q.-O. and D.C.-C. conceptualized the study. D.C.-C. and B. R.-M. designed methodology. M.D-F. and I.A-S collected, prepared and/or provided the clinical samples. D.C.-C. lead formal analyses. D.C.-C. and B.R-M. performed methodology. F.C., B.R-M. and D.C.-C. analyzed data. D.C.-C. provided software support. D.C.-C. performed data visualization with contributions from F.C., M.I.Q.-O., B.R.-M. and A.R-E. D.C.-C. wrote the original draft. M.I.Q.-O. and B.R-M is the guarantor of this work, has full access to all the data in the study and takes responsibility for the integrity of the data. All authors reviewed and edited the manuscript. All authors have read and agreed to the published version of the manuscript.

Consent for publication

Not applicable

Funding

This research was developed thank to the funding from the Institute of Health Carlos III (ISCIII) (PI18/00453, PI17/01104, PI20/00505 and PI23/00171), CTS981 (Andalusian Research, Develpment and Innovation Frame) and co-financed by the European Regional Development Fund (ERDF). BRM was supported by the "Miguel Servet Type I" program (CP19/00098) from the ISCIII. DCC was supported by the postdoctoral program "Sara Borrell" from the ISCIII (CD21/00164). All authors have read the journal's policy on disclosure of potential conflicts of interest and declare no conflict of interests.

CRediT authorship contribution statement

Fernando Cardona: Writing – review & editing, Visualization, Resources, Funding acquisition, Formal analysis, Conceptualization. **Armando Reyes-Engel:** Writing – review & editing, Visualization. **María Isabel Queipo-Ortuño:** Writing – review & editing, Visualization, Supervision, Conceptualization. **María Dolores Frutos:** Writing – review & editing, Resources. **Daniel Castellano-Castillo:** Writing – original draft, Visualization, Software, Methodology, Formal analysis, Data curation, Conceptualization. **Isabel Arranz-Salas:** Data curation, Methodology. **Bruno Ramos-Molina:** Writing – review & editing, Visualization, Supervision, Resources, Methodology, Formal analysis.

Declaration of Competing Interest

The authors declare that they have no known competing financial interests or personal relationships that could have appeared to influence the work reported in this paper.

Appendix A. Supporting information

Supplementary data associated with this article can be found in the online version at doi:10.1016/j.biopha.2024.116508.

References

[1] Z. Younossi, Q.M. Anstee, M. Marietti, T. Hardy, L. Henry, M. Eslam, J. George, E. Bugianesi, Global burden of NAFLD and NASH: trends, predictions, risk factors and prevention, 2017 151, Nat. Rev. Gastroenterol. Hepatol. 15 (2017) 11–20, https://doi.org/10.1038/nrgastro.2017.109.

[2] J. Quek, K.E. Chan, Z.Y. Wong, C. Tan, B. Tan, W.H. Lim, D.J.H. Tan, A.S.P. Tang, P. Tay, J. Xiao, J.N. Yong, R.W. Zeng, N.W.S. Chew, B. Nah, A. Kulkarni, M. S. Siddiqui, Y.Y. Dan, V.W.S. Wong, A.J. Sanyal, M. Noureddin, M. Muthiah, C. H. Ng, Global prevalence of non-alcoholic fatty liver disease and non-alcoholic steatohepatitis in the overweight and obese population: a systematic review and meta-analysis, Lancet Gastroenterol. Hepatol. 8 (2023) 20–30, https://doi.org/10.1016/S2468-1253(22)00317-X.

[3] P. Nasr, F. Iredahl, N. Dahlström, K. Rådholm, P. Henriksson, G. Cedersund, O. Dahlqvist Leinhard, T. Ebbers, J. Alfredsson, C.J. Carlhäll, P. Lundberg, S. Kechagias, M. Ekstedt, Evaluating the prevalence and severity of NAFLD in primary care: the EPSONIP study protocol, BMC Gastroenterol. 21 (2021) 1–11, https://doi.org/10.1186/S12876-021-01763-Z/TABLES/4.

[4] D. Castellano-Castillo, B. Ramos-Molina, F. Cardona, M.I. Queipo-Ortuño, Epigenetic regulation of white adipose tissue in the onset of obesity and metabolic diseases, Obes. Rev. 21 (2020) e13054, https://doi.org/10.1111/obr.13054.

[5] V. Woo, T. Alenghat, Epigenetic regulation by gut microbiota, (2022). https://doi.org/10.1080/19490976.2021.2022407.

[6] K.A. Tran, C.M. Dillingham, R. Sridharan, The role of α-ketoglutarate–dependent proteins in pluripotency acquisition and maintenance, J. Biol. Chem. 294 (2019) 5408, https://doi.org/10.1074/JBC.TM118.000831.

[7] M. Xiao, H. Yang, W. Xu, S. Ma, H. Lin, H. Zhu, L. Liu, Y. Liu, C. Yang, Y. Xu, S. Zhao, D. Ye, Y. Xiong, K.L. Guan, Inhibition of α-KG-dependent histone and DNA demethylases by fumarate and succinate that are accumulated in mutations of FH and SDH tumor suppressors, Genes Dev. 26 (2012) 1326–1338, https://doi.org/10.1101/GAD.191056.112.

[8] Z. Dai, V. Ramesh, J.W. Locasale, The evolving metabolic landscape of chromatin biology and epigenetics, Nat. Rev. Genet. 21 (2020) 737–753, https://doi.org/10.1038/S41576-020-0270-8.

[9] J.D. Buenrostro, B. Wu, H.Y. Chang, W.J. Greenleaf, ATAC-seq: a method for assaying chromatin accessibility genome-wide, 21.29.1, Curr. Protoc. Mol. Biol. 109 (2015), https://doi.org/10.1002/0471142727.MB2129S109.

[10] P. Bedossa, C. Poitou, N. Veyrie, J.L. Bouillot, A. Basdevant, V. Paradis, J. Tordjman, K. Clement, Histopathological algorithm and scoring system for evaluation of liver lesions in morbidly obese patients, Hepatology 56 (2012) 1751–1759, https://doi.org/10.1002/hep.25889.

[11] F. Yan, D.R. Powell, D.J. Curtis, N.C. Wong, From reads to insight: a hitchhiker's guide to ATAC-seq data analysis, 2020 211. Genome Biol. 21 (2020) 1–16, https://doi.org/10.1186/S13059-020-1929-3.

[12] J.J. Reske, M.R. Wilson, R.L. Chandler, ATAC-seq normalization method can significantly affect differential accessibility analysis and interpretation, Epigenetics Chromatin 13 (2020) 22, https://doi.org/10.1186/s13072-020-00342-y.

[13] T. Gao, J. Qian, EnhancerAtlas 2.0: an updated resource with enhancer annotation in 586 tissue/cell types across nine species, Nucleic Acids Res. 48 (2020) D58–D64, https://doi.org/10.1093/NAR/GKZ980.

[14] A. Khan, X. Zhang, dbSUPER: a database of super-enhancers in mouse and human genome, Nucleic Acids Res. 44 (2016) D164–D171, https://doi.org/10.1093/NAR/GKV1002.

[15] N. Sodum, G. Kumar, S.L. Bojja, N. Kumar, C.M. Rao, Epigenetics in NAFLD/NASH: targets and therapy, Pharmacol. Res. 167 (2021) 105484, https://doi.org/10.1016/J.PHRS.2021.105484.
[16] D.A. Pollyea, C.D. DiNardo, M.L. Arellano, A. Pigneux, W. Fiedler, M. Konopleva, D.A. Rizzieri, B.D. Smith, A. Shinagawa, R.M. Lemoli, M. Dail, Y. Duan, B. Chyla, J. Potluri, C.L. Miller, H.M. Kantarjian, Impact of venetoclax and azacitidine in treatment-naïve patients with acute Myeloid Leukemia and IDH1/2 mutations, Clin. Cancer Res. 28 (2022) 2753–2761, https://doi.org/10.1158/1078-0432.CCR-21-3467.
[17] A. Bazinet, F. Darbaniyan, E. Jabbour, G. Montalban-Bravo, M. Ohanian, K. Chien, T. Kadia, K. Takahashi, L. Masarova, N. Short, Y. Alvarado, M. Yilmaz, F. Ravandi, M. Andreeff, R. Kanagal-Shamanna, I. Ganan-Gomez, S. Colla, W. Qiao, X. Huang, D. McCue, B. Mirabella, H. Kantarjian, G. Garcia-Manero, Azacitidine plus venetoclax in patients with high-risk myelodysplastic syndromes or chronic myelomonocytic leukaemia: phase 1 results of a single-centre, dose-escalation, dose-expansion, phase 1–2 study, Lancet Haematol. 9 (2022) e756–e765, https://doi.org/10.1016/S2352-3026(22)00216-2.
[18] K. Tao, Y. Inamoto, H. Furukawa, R. Hosoba, W. Takeda, A. Maeshima, J. Aoki, A. Ito, T. Tanaka, S.W. Kim, S. Makita, S. Fukuhara, Y. Kogure, K. Kataoka, K. Izutsu, T. Fukuda, Romidepsin-induced durable remission for relapsed nodal peripheral T-cell lymphoma with T follicular helper phenotype after allogeneic hematopoietic cell transplantation, Int. J. Hematol. (2023), https://doi.org/10.1007/s12185-023-03561-7.
[19] D. Shafer, A.B. Kagan, M.A. Rudek, M. Kmieciak, M.B. Tombes, E. Shrader, D. Bandyopadhyay, D. Hudson, H. Sankala, C. Weir, J.E. Lancet, S. Grant, Phase 1 study of belinostat and adavosertib in patients with relapsed or refractory myeloid malignancies, Cancer Chemother. Pharmacol. 91 (2023) 281–290, https://doi.org/10.1007/s00280-023-04511-0.
[20] V.R. Muñoz, R.C. Gaspar, G.K. Kuga, A.L. da Rocha, B.M. Crisol, J.D. Botezelli, I. L. Baptista, R.A. Mekary, A.S.R. da Silva, D.E. Cintra, L.P. de Moura, E.R. Ropelle, J.R. Pauli, Exercise increases Rho-kinase activity and insulin signaling in skeletal muscle, J. Cell. Physiol. 233 (2018) 4791–4800, https://doi.org/10.1002/jcp.26278.
[21] A. Chadt, H. Al-Hasani, Glucose transporters in adipose tissue, liver, and skeletal muscle in metabolic health and disease, Pflug. Arch. Eur. J. Physiol. 472 (2020) 1273–1298, https://doi.org/10.1007/s00424-020-02417-x.
[22] N. Boudaba, A. Marion, C. Huet, R. Pierre, B. Viollet, M. Foretz, AMPK re-activation suppresses hepatic steatosis but its downregulation does not promote fatty liver development, EBioMedicine 28 (2018) 194–209, https://doi.org/10.1016/j.ebiom.2018.01.008.
[23] P. Zhao, X. Sun, C. Chaggan, Z. Liao, K. in Wong, F. He, S. Singh, R. Loomba, M. Karin, J.L. Witztum, A.R. Saltiel, An AMPK–caspase-6 axis controls liver damage in nonalcoholic steatohepatitis, Science 367 (80-.) (2020) 652–660, https://doi.org/10.1126/science.aay0542.
[24] J. Pu, Targeting the lysosome: mechanisms and treatments for nonalcoholic fatty liver disease, J. Cell. Biochem. 123 (2022) 1624–1633, https://doi.org/10.1002/jcb.30274.
[25] S. Lee, H.H. Dong, FoxO integration of insulin signaling with glucose and lipid metabolism, J. Endocrinol. 233 (2017) R67–R79, https://doi.org/10.1530/JOE-17-0002.
[26] X. Pan, Y. Zhang, H.G. Kim, S. Liangpunsakul, X.C. Dong, FOXO transcription factors protect against the diet-induced fatty liver disease, Sci. Rep. 7 (2017) 1–12, https://doi.org/10.1038/srep44597.
[27] A. Moslehi, Z. Hamidi-zad, Role of SREBPs in liver diseases: a mini-review, J. Clin. Transl. Hepatol. 6 (2018) 332–338, https://doi.org/10.14218/JCTH.2017.00061.
[28] T. Nagaya, N. Tanaka, T. Suzuki, K. Sano, A. Horiuchi, M. Komatsu, T. Nakajima, T. Nishizawa, S. Joshita, T. Umemura, T. Ichijo, A. Matsumoto, K. Yoshizawa, J. Nakayama, E. Tanaka, T. Aoyama, Down-regulation of SREBP-1c is associated with the development of burned-out NASH, J. Hepatol. 53 (2010) 724–731, https://doi.org/10.1016/j.jhep.2010.04.033.
[29] P. Heitel, G. Faudone, M. Helmstädter, J. Schmidt, A. Kaiser, A. Tjaden, M. Schröder, S. Müller, S. Schierle, J. Pollinger, D. Merk, A triple farnesoid X receptor and peroxisome proliferator-activated receptor α/δ activator reverses hepatic fibrosis in diet-induced NASH in mice, Commun. Chem. 3 (2020) 1–16, https://doi.org/10.1038/s42004-020-00411-z.
[30] T.T.P. Nguyen, D.Y. Kim, Y.G. Lee, Y.S. Lee, X.T. Truong, J.H. Lee, D.K. Song, T. K. Kwon, S.H. Park, C.H. Jung, C. Moon, T.F. Osborne, S.S. Im, T.Il Jeon, SREBP-1c impairs ULK1 sulfhydration-mediated autophagic flux to promote hepatic steatosis in high-fat-diet-fed mice, 3820-3832.e7, Mol. Cell. 81 (2021), https://doi.org/10.1016/j.molcel.2021.06.003.
[31] X. Li, G. Egervari, Y. Wang, S.L. Berger, Z. Lu, Regulation of chromatin and gene expression by metabolic enzymes and metabolites, 2018 199. 19, Nat. Rev. Mol. Cell Biol. (2018) 563–578, https://doi.org/10.1038/s41580-018-0029-7.
[32] Q. Su, S.Y. Kim, F. Adewale, Y. Zhou, C. Aldler, M. Ni, Y. Wei, M.E. Burczynski, G. S. Atwal, M.W. Sleeman, A.J. Murphy, Y. Xin, X. Cheng, Single-cell RNA transcriptome landscape of hepatocytes and non-parenchymal cells in healthy and NAFLD mouse liver, IScience 24 (2021), https://doi.org/10.1016/j.isci.2021.103233.
[33] S.A. MacParland, J.C. Liu, X.Z. Ma, B.T. Innes, A.M. Bartczak, B.K. Gage, J. Manuel, N. Khuu, J. Echeverri, I. Linares, R. Gupta, M.L. Cheng, L.Y. Liu, D. Camat, S. W. Chung, R.K. Seliga, Z. Shao, E. Lee, S. Ogawa, M. Ogawa, M.D. Wilson, J.E. Fish, M. Selzner, A. Ghanekar, D. Grant, P. Greig, G. Sapisochin, N. Selzner, N. Winegarden, O. Adeyi, G. Keller, G.D. Bader, I.D. McGilvray, Single cell RNA sequencing of human liver reveals distinct intrahepatic macrophage populations, Nat. Commun. 9 (2018) 1–21, https://doi.org/10.1038/s41467-018-06318-7.
[34] D. Cheng, J. Chai, H. Wang, L. Fu, S. Peng, X. Ni, Hepatic macrophages: key players in the development and progression of liver fibrosis, Liver Int 41 (2021) 2279–2294, https://doi.org/10.1111/LIV.14940.
[35] M.P. Suppli, K.T.G. Rigbolt, S.S. Veidal, S. Heebøll, P.L. Eriksen, M. Demant, J. I. Bagger, J.C. Nielsen, D. Oró, S.W. Thrane, A. Lund, C. Strandberg, M.J. Kønig, T. Vilsbøll, N. Vrang, K.L. Thomsen, H. Grønbæk, J. Jelsing, H.H. Hansen, F. K. Knop, Hepatic transcriptome signatures in patients with varying degrees of nonalcoholic fatty liver disease compared with healthy normal-weight individuals, Am. J. Physiol. - Gastrointest. Liver Physiol. 316 (2019) G462–G472, https://doi.org/10.1152/ajpgi.00358.2018.
[36] T. Varga, Z. Czimmerer, L. Nagy, PPARs are a unique set of fatty acid regulated transcription factors controlling both lipid metabolism and inflammation, Biochim. Biophys. Acta - Mol. Basis Dis. 1812 (2011) 1007–1022, https://doi.org/10.1016/J.BBADIS.2011.02.014.
[37] R.M. Salama, S.S. Abbas, S.F. Darwish, A.A. Sallam, N.F. Elmongy, S.A. El Wakeel, Regulation of NOX/p38 MAPK/PPARα pathways and miR-155 expression by boswellic acids reduces hepatic injury in experimentally-induced alcoholic liver disease mouse model: novel mechanistic insight, Arch. Pharm. Res. 46 (2023) 323–338, https://doi.org/10.1007/s12272-023-01441-6.
[38] R.-N. Zhang, F. Shen, Q. Pan, H.-X. Cao, G.-Y. Chen, J.-G. Fan, PPARGC1A rs8192678 G>A polymorphism affects the severity of hepatic histological features and nonalcoholic steatohepatitis in patients with nonalcoholic fatty liver disease. World J. Gastroenterol. 27 (2021) 3863–3876, https://doi.org/10.3748/wjg.v27.i25.3863.
[39] Y. Jiang, D. Chen, Q. Gong, Q. Xu, D. Pan, F. Lu, Q. Tang, Elucidation of SIRT-1/PGC-1α-associated mitochondrial dysfunction and autophagy in nonalcoholic fatty liver disease, Lipids Health Dis. 20 (2021) 40, https://doi.org/10.1186/s12944-021-01461-5.
[40] T.A. Christiansen-Weber, J.R. Voland, Y. Wu, K. Ngo, B.L. Roland, S. Nguyen, P. A. Peterson, W.P. Fung-Leung, Functional loss of ABCA1 in mice causes severe placental malformation, aberrant lipid distribution, and kidney glomerulonephritis as well as high-density lipoprotein cholesterol deficiency, Am. J. Pathol. 157 (2000) 1017–1029, https://doi.org/10.1016/S0002-9440(10)64614-7.
[41] C.-C.C. Key, M. Liu, C.L. Kurtz, S. Chung, E. Boudyguina, T.A. Dinh, A. Bashore, P. E. Phelan, B.I. Freedman, T.F. Osborne, X. Zhu, L. Ma, P. Sethupathy, S. B. Biddinger, J.S. Parks, Hepatocyte ABCA1 deletion impairs liver insulin signaling and lipogenesis, Cell Rep. 19 (2017) 2116–2129, https://doi.org/10.1016/j.celrep.2017.05.032.
[42] M.J. Akhtar, S.A. Khan, B. Kumar, P. Chawla, R. Bhatia, K. Singh, Role of sodium dependent SLC13 transporter inhibitors in various metabolic disorders, Mol. Cell. Biochem. 478 (2023) 1669–1687, https://doi.org/10.1007/s11010-022-04618-7.
[43] J. Remetic, A. Ghallab, Z. Hobloss, L. Brackhagen, R. Hassan, M. Myllys, R. Radun, V. Mlitz, C. Zhu, M. Baumgartner, W.C. Schrottmaier, M. Mussbacher, G. Timelthaler, H. Scharnagl, T. Stojakovic, A. Assinger, C.D. Fuchs, J.G. Hengstler, M. Trauner, Loss of bile salt export pump aggravates lipopolysaccharide-induced liver injury in mice due to impaired hepatic endotoxin clearance, Hepatology 75 (2022) 1095–1109, https://doi.org/10.1002/hep.32289.
[44] C. Jouffe, B.D. Weger, E. Martin, F. Atger, M. Weger, C. Gobet, D. Ramnath, A. Charpagne, D. Morin-Rivron, E.E. Powell, M.J. Sweet, M. Masoodi, N. H. Uhlenhaut, F. Gachon, Disruption of the circadian clock component BMAL1 elicits an endocrine adaption impacting on insulin sensitivity and liver disease, Proc. Natl. Acad. Sci. U. S. A. 119 (2022) e2200083119, https://doi.org/10.1073/pnas.2200083119.
[45] L. Xu, T.-Y. Yang, Y.-W. Zhou, M.-F. Wu, J. Shen, J.-L. Cheng, Q.-X. Liu, S.-Y. Cao, J.-Q. Wang, L. Zhang, Bmal1 inhibits phenotypic transformation of hepatic stellate cells in liver fibrosis via IDH1/α-KG-mediated glycolysis, Acta Pharmacol. Sin. 43 (2022) 316–329, https://doi.org/10.1038/s41401-021-00658-9.
[46] J.M. Mellado-Gil, E. Fuente-Martín, P.I. Lorenzo, N. Cobo-Vuilleumier, L. López-Noriega, A. Martín-Montalvo, I.D.G.H. Gómez, M. Ceballos-Chávez, L. Gómez-Jaramillo, A. Campos-Caro, S.Y. Romero-Zerbo, J. Rodríguez-Comas, J.M. Servitja, G. Rojo-Martinez, A. Hmadcha, B. Soria, M. Bugliani, P. Marchetti, F.J. Bérmudez-Silva, J.C. Reyes, M. Aguilar-Diosdado, B.R. Gauthier, The type 2 diabetes-associated HMG20A gene is mandatory for islet beta cell functional maturity, Cell Death Dis. 9 (2018), https://doi.org/10.1038/S41419-018-0272-Z.
[47] X.-K. Wang, X.-W. Liao, X. Zhou, C.-Y. Han, Z.-J. Chen, C.-K. Yang, J.-L. Huang, J.-Y. Wang, J.-Q. Liu, H.-S. Huang, S.-T. Mo, X.-P. Ye, G.-Z. Zhu, T. Peng, Oncogene UBE2I enhances cellular invasion, migration and proliferation abilities via autophagy-related pathway resulting in poor prognosis in hepatocellular carcinoma, Am. J. Cancer Res. 10 (2020) 4178. /pmc/articles/PMC7783760/ (accessed March 16, 2023).
[48] M. O'Farrell, G. Duke, R. Crowley, D. Buckley, E.B. Martins, D. Bhattacharya, S. L. Friedman, G. Kemble, FASN inhibition targets multiple drivers of NASH by reducing steatosis, inflammation and fibrosis in preclinical models, 2022 121. 12, Sci. Rep. (2022) 1–16, https://doi.org/10.1038/s41598-022-19459-z.
[49] R. Loomba, R. Mohseni, K.J. Lucas, J.A. Gutierrez, R.G. Perry, J.F. Trotter, R. S. Rahimi, S.A. Harrison, V. Ajmera, J.D. Wayne, M. O'Farrell, W. McCulloch, K. Grimmer, M. Rinella, V. Wai-Sun Wong, V. Ratziu, G.J. Gores, B. A. Neuschwander-Tetri, G. Kemble, TVB-2640 (FASN Inhibitor) for the treatment of nonalcoholic steatohepatitis: FASCINATE-1, a randomized, placebo-controlled phase 2a Trial, Gastroenterology 161 (2021) 1475–1486, https://doi.org/10.1053/j.gastro.2021.07.025.
[50] M. Domínguez-Pérez, A. Simoni-Nieves, P. Rosales, N. Nuño-Lámbarri, M. Rosas-Lemus, V. Souza, R.U. Miranda, L. Bucio, S. Uribe Carvajal, J.U. Marquardt, D. Seo, L.E. Gomez-Quiroz, M.C. Gutiérrez-Ruiz, Cholesterol burden in the liver induces mitochondrial dynamic changes and resistance to apoptosis, J. Cell. Physiol. 234 (2019) 7213–7223, https://doi.org/10.1002/JCP.27474.

[51] Y.A. An, S. Chen, Y. Deng, Z.V. Wang, J.B. Funcke, M. Shah, B. Shan, R. Gordillo, J. Yoshino, S. Klein, C.M. Kusminski, P.E. Scherer, The mitochondrial dicarboxylate carrier prevents hepatic lipotoxicity by inhibiting white adipocyte lipolysis, J. Hepatol. 75 (2021) 387–399, https://doi.org/10.1016/J.JHEP.2021.03.006.

[52] J.S. Bogan, S.K. Shenoy, N.J. Grimsey, N.J. Hoffman, Ubiquitin-like processing of TUG proteins as a mechanism to regulate glucose uptake and energy metabolism in fat and muscle OPEN ACCESS EDITED BY, Front. Endocrinol. 13 (2022) 1019405, https://doi.org/10.3389/fendo.2022.1019405.

[53] J.S. Bogan, N. Hendon, A.E. McKee, T.S. Tsao, H.F. Lodish, Functional cloning of TUG as a regulator of GLUT4 glucose transporter trafficking, 2003 4256959, Nature 425 (2003) 727–733, https://doi.org/10.1038/nature01989.

[54] M.D. Fullerton, F. Hakimuddin, A. Bonen, M. Bakovic, The development of a metabolic disease phenotype in CTP:phosphoethanolamine cytidylyltransferase-deficient mice, J. Biol. Chem. 284 (2009) 25704–25713, https://doi.org/10.1074/JBC.M109.023846.

[55] S. Grapentine, R.K. Singh, P. Basu, S. Sivanesan, G. Mattos, O. Oresajo, J. Cheema, W. Demeke, V.W. Dolinsky, M. Bakovic, Pcyt2 deficiency causes age-dependant development of nonalcoholic steatohepatitis and insulin resistance that could be attenuated with phosphoethanolamine, 2022 121, Sci. Rep. 12 (2022) 1–17, https://doi.org/10.1038/s41598-022-05140-y.

[56] X. Hang, Z. Wu, K. Chu, G. Yu, H. Peng, H. Xin, X. Miao, J. Wang, W. Xu, Low expression of DCXR protein indicates a poor prognosis for hepatocellular carcinoma patients, Tumour Biol. 37 (2016) 15079–15085, https://doi.org/10.1007/S13277-016-5302-9.

[57] M. Sakaguchi, W. Cai, C.H. Wang, C.T. Cederquist, M. Damasio, E.P. Homan, T. Batista, A.K. Ramirez, M.K. Gupta, M. Steger, N.J. Wewer Albrechtsen, S. K. Singh, E. Araki, M. Mann, S. Enerbäck, C.R. Kahn, FoxK1 and FoxK2 in insulin regulation of cellular and mitochondrial metabolism, 2019 101. Nat. Commun. 10 (2019) 1–17, https://doi.org/10.1038/s41467-019-09418-0.

[58] M.L. Boland, R.C. Laker, K. Mather, A. Nawrocki, S. Oldham, B.B. Boland, H. Lewis, J. Conway, J. Naylor, S. Guionaud, M. Feigh, S.S. Veidal, L. Lantier, O. P. McGuinness, J. Grimsby, C.M. Rondinone, L. Jermutus, M.R. Larsen, J. L. Trevaskis, C.J. Rhodes, Resolution of NASH and hepatic fibrosis by the GLP-1R/GcgR dual-agonist Cotadutide via modulating mitochondrial function and lipogenesis, Nat. Metab. 2 (2020) 413, https://doi.org/10.1038/S42255-020-0209-6.

[59] M. Remely, E. Aumueller, C. Merold, S. Dworzak, B. Hippe, J. Zanner, A. Pointner, H. Brath, A.G. Haslberger, Effects of short chain fatty acid producing bacteria on epigenetic regulation of FFAR3 in type 2 diabetes and obesity, Gene 537 (2014) 85–92, https://doi.org/10.1016/j.gene.2013.11.081.

[60] X.S. Liu, H. Wu, X. Ji, Y. Stelzer, X. Wu, S. Czauderna, J. Shu, D. Dadon, R. A. Young, R. Jaenisch, Editing DNA Methylation in the Mammalian Genome, Cell (2016), https://doi.org/10.1016/j.cell.2016.08.056.

[61] J. Pulecio, N. Verma, E. Mejía-Ramírez, D. Huangfu, A. Raya, CRISPR/Cas9-based engineering of the epigenome, Cell Stem Cell 21 (2017) 431, https://doi.org/10.1016/J.STEM.2017.09.006.

[62] H. O'Geen, S.L. Bates, S.S. Carter, K.A. Nisson, J. Halmai, K.D. Fink, S.K. Rhie, P. J. Farnham, D.J. Segal, Ezh2-dCas9 and KRAB-dCas9 enable engineering of epigenetic memory in a context-dependent manner, Epigenetics Chromatin 12 (2019), https://doi.org/10.1186/S13072-019-0275-8.